Biochimica et Biophysica Acta, 1024 (1990) 373–379
Elsevier

BBAMEM 74834

Time course analysis of cotransport in membrane vesicles: solutes and tracers

F. Andrietti [1], A. Della Torre Piccinelli [1] and V.F. Sacchi [2]

[1] *Dipartimento di Biologia and* [2] *Istituto di Fisiologia Generale e Chimica Biologica, Università di Milano, Milano (Italy)*

(Received 15 August 1989)
(Revised manuscript received 25 January 1990)

Key words: Cotransport model; Computer simulation; Isotope tracer; Membrane vesicle

A theoretical analysis of the time course of a ternary cotransport system in membrane vesicles has been developed by extending previous work (Weiss, S.D. et al. (1981) J. Theor. Biol. 93, 597–608; Heinz, E. and Weinstein, M. (1984) Biochim. Biophys. Acta 776, 83–91). It has been assumed that the translocation of the carrier is the rate-limiting step of the transport process. Our approach includes, in particular, the presence of isotope tracer fluxes and the generalization to the case when many solutes share the same carrier. The situation when the tracer and the solute behave differently, as in the countertransport case, is stressed. Also, the interaction of two different solutes, internal and external to vesicles, is considered. Other points regard the analysis of the solute binding to the membrane vesicles, the influence of water permeability and the possible asymmetry of the transport system. In the Appendix, the assumption of no net translocation of all carrier species is discussed.

Introduction

The theory presented here regards the uptake time course of cotransported solutes in membrane vesicles. Previous investigations in this direction were made by Weiss et al. [1] and Heinz and Weinstein [2]. We will assume as in Ref. 2 that only ternary complexes are formed and that the binding sequence of driver and solute is random. Our line of reasoning is close to that followed by Heinz and Weinstein [2], but our attempt has been extended to include the flux of isotope tracers, the effect of water permeability and that of asymmetric membranes. In addition, our model takes into account more than one solute sharing the same transport system and the presence of possible binding of the cotransported solute to the vesicular membrane.

Instead, we will not consider different cases, in which the activator must bind before or after the solute, like those examined by Turner [3] and Turner and Silverman [4] for initial solute uptakes.

Correspondence: F. Andrietti, Dipartimento di Biologia, Università di Milano, I-20133 Milano, Italy.

Glossary

a_i', a_i'': activity of i-th solute (mM);
b', b'': activity of a monovalent driver cation (mM);
x', x'': amount of unloaded carrier per g protein (μmol $\cdot g^{-1}$);
X_T: total amount of carrier per g protein ($\mu mol \cdot g^{-1}$);
$(a_i b^{n_i} x)'$, $(a_i b^{n_i} x)''$: amount of i-th ternary complex ($\mu mol \cdot g^{-1}$);
s', s'': activity of impermeant solute (mM);
r_v: vesicular radius (cm);
P_{D_i}: permeability constant for i-th solute free diffusion ($ml \cdot g^{-1} \cdot min^{-1}$);
P_+: cation permeability of the driver salt ($ml \cdot g^{-1} \cdot min^{-1}$);
P_s: permeability of the driver salt ($ml \cdot g^{-1} \cdot min^{-1}$);
W: vesicular volume per g protein ($ml \cdot g^{-1}$);
P_0: rate coefficient of empty carrier translocation (min^{-1});
P_i ($= \alpha_i P_0$): rate coefficient of translocation of i-th ternary complex (min^{-1});
K_i: dissociation constant of i-th ternary complex (mM^2);
n_i: stoichiometry coefficient;
μ: electrochemical activity coefficient;
r: ratio of cation over anion permeability of the permeant salt;

α_i: ratio of rate coefficient of the translocation of the i-th ternary complex over the unloaded carrier;
K', K'': dissociation constants in asymmetric membranes;
P_0', P_0'': rate coefficients of carrier translocation in asymmetric membranes;
P', P'': rate coefficients of complex translocation in asymmetric membranes.

Formulation of the general model

The general model here considered does not make any assumption on the mechanism by which the solutes are transported. It consists of a system of differential equations describing:

(1) The rate of change of solute quantity Wa_i'' inside membrane vesicles given by

$$d/dt(Wa_i'') = (J_i' - J_i'') + P_{Di}(a_i' - a_i'') \quad (1)$$

where the first component in the right hand side of Eqn. 1 is the difference of undirectional influx J_i' and efflux J_i'' due to the carrier mediated transport, while the second term is a diffusional component with a permeability coefficient P_{Di}; W is the vesicular volume.

(2) The rate of change of internal driver concentration b'', supposed to be controlled by a diffusional process only, with a permeability coefficient P_S, since the contribution cotransported with the carrier is negligible. It will be expressed by

$$d/dt(Wb'') = P_S(b' - b'') \quad (2)$$

P_S is related to the ratio $r = P_+/P_-$ of cation over the anion permeability by $P_S = [2/(r+1)]P_+$ [2].

(3) The rate of change of the vesicular radius r_v (vesicles are supposed to be spherical), due to water movement. It will be given by

$$dr_v/dt = P_W\left(2b'' + \sum a_i'' + s'' - 2b' - \sum a_i' - s'\right)(r_v^2(0)/r_v^2) \quad (3)$$

where P_W is the water osmotic permeability, s' and s'' are the external and internal concentrations of any impermeant solute and $r_v(0)$ is the initial value of r_v. The factor 2 takes into account that the driver ion diffuses as a binary salt. It is assumed that during water flux the vesicles surface $4\pi r_v^2(0)$ remains unchanged.

(4) The rate of change of the quantity $^*Q_i = W{}^*a_i''$, i.e., the tracer present inside the vesicles. The unidirectional isotope flux across the vesicle walls will be given by the unidirectional fluxes of the solute times the ratio between isotope and solute concentrations. So one finds

$$d{}^*Q_i/dt = [({}^*a_i'/a_i')J_i' - ({}^*a_i''/a_i'')J_i''] + P_{Di}({}^*a_i' - a_i'') \quad (4)$$

where $^*a_i'$ and $^*a_i''$ are the external and internal isotope concentrations.

To determine the total radioactivity $^*R_i$ present in vesicles, a possible contribution of isotope $^*B_i$ bound to the membrane has to be added to that inside the vesicles

$$^*R_i = {}^*Q_i + {}^*B_i \quad (5)$$

In order to proceed to the integration of Eqns. 1–4, with the possible contribution of Eqn. 5, an evaluation of J_i has to be found, according to the different models of transport that may be considered.

Ternary complex model: theory and simulation

The ternary complex model that we consider here is a generalization of that reported by Heinz and Weinstein [2], under the assumption that the carrier translocation is rate limiting. This choice corresponds to that of most authors even if an alternative approach in which association and dissociation constants are rate limiting may not be ruled out (see, for example, Refs. 2 and 5). Besides, this is the situation found for valinomycin, that may be considered as a typical mobile carrier system [6]. However, the analysis presented here could be easily extended to the case when binding of the solutes to the carrier is the rate-limiting step.

When the two sides of the membrane are symmetric and the association and dissociation reactions between empty carrier (x), ligand solutes (a_i) and driver ion (b) are very fast, as compared with translocation of the carrier species, we may write the (quasi) equilibrium conditions

$$a_i'(b')^{n_i}x/(a_ib^{n_i}x)' = K_i = a_i''(b'')^{n_i}x''/(a_ib^{n_i}x)'' \quad (6)$$

where n_i is the stoichiometry ratio of the driver ion/solute and K_i is the dissociation constant of the ternary complex ($a_ib^{n_i}x$).

If, moreover, the sum X_T of all carrier species remains the same, one has

$$x' + x''\sum_i (a_ib^{n_i}x)' + \sum_i (a_ib^{n_i}x)'' = X_T \quad (7)$$

where the tracers are not taken into account since their contribution is negligible.

The flux of all carrier species in opposite directions is approximately the same if changes in carrier species distribution may be neglected. In the Appendix it is shown that this assumption holds when the total amount of carrier is less than 1 μmol per gram of vesicular protein.

Taking into account the possible influence of a transmembrane electrical potential difference, the last assumption yields

$$\sum_i P_i(ab^{n_i}x)'\mu^{n_i/2} + P_0x' = \sum_i P_i(ab^{n_i}x)''\mu^{-n_i/2} + P_0x'' \quad (8a)$$

when the empty carrier bears no charge, and

$$\sum_i P_i(ab^{n_i}x)' + P_0x'\mu^{-n_i/2} = \sum_i P_i(ab^{n_i}x)'' + P_0x''\mu^{n_i/2} \quad (8b)$$

when the empty carrier bears a charge opposite to that of the driver ion times its stoichiometry ratio. The value of μ (electrochemical activity coefficient) may be calculated according to Henderson or Goldman and Hodgkin equations (see Ref. 2).

The value of J_i fluxes may be found according to the previous equations. Since calculations become cumbersome with increasing numbers of solutes, we give the results only for $i = 1, 2$. In this case from Eqns. 6–8a one has

$$x'' = K_1K_2X_T[K_1K_2 + K_2a_1'(b')^{n_1}\alpha_1\mu^{n_1/2} + K_1a_2'(b')^{n_2}\alpha_2\mu^{n_2/2}]/\{\} \quad (9)$$

$$x' = K_1K_2X_T[K_1K_2 + K_2a_1''(b'')^{n_1}\alpha_1\mu^{-n_1/2} + K_1a_2''(b'')^{n_2}\alpha_2\mu^{-n_2/2}]/\{\} \quad (10)$$

where

$$\begin{aligned}\{\} = {} & 2(K_2)^2(K_1)^2 + a_1'(b')^{n_1}(1+\alpha_1\mu^{n_1/2})K_1(K_2)^2 \\ & + a_1''(b'')^{n_1}(K_2)^2[(1+\alpha_1\mu^{-n_1/2})K_1 \\ & + (\mu^{n_1/2}+\mu^{-n_1/2})\alpha_1a_1'(b')^{n_1}] \\ & + a_2'(b')^{n_2}(1+\alpha_2\mu^{n_2/2})(K_1)^2K_2 + a_2''(b'')^{n_2}(K_1)^2 \\ & \times[(1+\alpha_2\mu^{-n_2/2})K_2 + (\mu^{n_2/2}+\mu^{-n_2/2})\alpha_2a_2'(b')^{n_2}] \\ & + K_1K_2a_1''(b'')^{n_1}/a_2'(b')^{n_2} \\ & \times(\alpha_1\mu^{-n_1/2} + \alpha_2\mu^{n_2/2}) \\ & + K_1K_2a_1'(b')^{n_1}a_2''(b'')^{n_2}(\alpha_1\mu^{n_1/2} + \alpha_2\mu^{-n_2/2}) \end{aligned} \quad (11)$$

and $\alpha_i = P_i/P_0$.

For the sake of brevity, we omit here the analogous relations obtained from Eqns. 6–8b and we limit our study to the situation when the empty carriers bears no charge.

The value of J_i' is

$$J_i' = P_i(a_ib^{n_i}x)'\mu^{n_i/2} \quad (12a)$$

Analogously one obtains the values of J''

$$J_i'' = P_i(a_ib^{n_i}x)''\mu^{-n_i/2} \quad (12b)$$

Substituting Eqn. 10 in the expression of J_i' given by Eqns. 12a and 9 in Eqn. 12b and taking into account Eqn. 6 one finds

$$\begin{aligned} J_1 = {} & J_1' - J_1'' \\ = {} & \alpha_1P_0X_TK_1K_2\{a_1'(b')^{n_1}[\mu^{n_1/2}K_2 + a_2''(b'')^{n_2}\alpha_2\mu^{(n_1-n_2)/2}] \\ & - a_1''(b'')^{n_1}[\mu^{-n_1/2}K_2 + a_2'(b')^{n_2}\alpha_2\mu^{(n_2-n_1)/2}]\}/\{\} \end{aligned} \quad (13)$$

while J_2 may be found by interchanging the index 1 with 2 in Eqn. 13.

The tracer flux will be found according to Eqn. 4. One obtains

$$\begin{aligned} {}^*J_1 = {} & \alpha_1P_0X_TK_1K_2\{{}^*a_1'(b')^{n_1}[\mu^{n_1/2}K_2 + a_2''(b'')^{n_2}\alpha_2\mu^{(n_1-n_2)/2}] \\ & - {}^*a_1''(b'')^{n_1}[\mu^{-n_1/2}K_2 + a_2'(b')^{n_2}\alpha_2\mu^{(n_2-n_1)/2}] \\ & + [{}^*a'_1(b')^{n_1}a_1''(b'')^{n_1} - {}^*a_1''(b'')^{n_1}a_1'(b')^{n_1}]\alpha_1(K_2/K_1)]\}/\{\} \end{aligned} \quad (14)$$

while ${}^*J_2$ will be found by interchanging the index 1 with 2 in Eqn. 14.

Letting $a_2' = a_2'' = 0$, Eqn. 13 reduces to Eqn. A-6a of Ref. 2 and, after division by $(K_2)^2$, the tracer flux becomes by Eqn. 14

$${}^*J_1 = \alpha_1P_0X_T\{[{}^*a_1'(b')^{n_1}\mu^{n_1/2} - {}^*a_1''(b'')^{n_1}\mu^{-n_1/2}]K_1 + [{}^*a_1'(b')^{n_1}a_1''(b'')^{n_1} - {}^*a_1''(b'')^{n_1}a_1'(b')^{n_1}]\alpha_1]\}/\{\}^0 \quad (15)$$

where $\{\}^0$ is the same expression that we find in the denominator of Eqn. A-6a of Ref. 2.

Observe that Eqn. 14 may not be obtained simply by substituting ${}^*a_1$ to a_1 in Eqn. 13, since the last term in square brakets in the numerator of Eqn. 14 is not present in Eqn. 13. This means that in certain situations

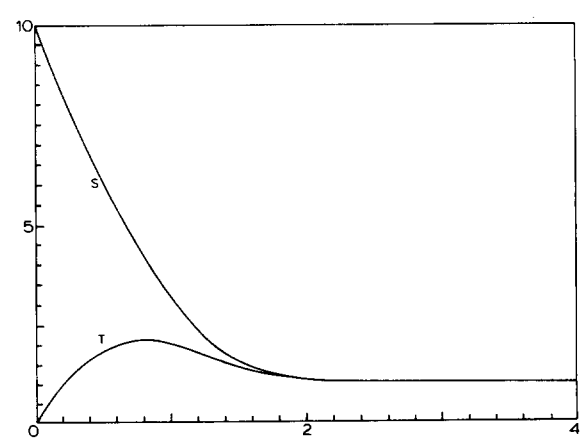

Fig. 1. Uptake curves of a solute (S) and its tracer (T) in a counter-transport simulation; the distribution ratios inside/outside the vesicles of both species (a_1''/a_1' or ${}^*a_1''/{}^*a_1'$) are plotted vs. time. Initial internal values: $a_1''(0) = 1$ mM, $b''(0) = 100$ mM. The other parameter values are given in Table I.

TABLE I

Standard values

P_+	2 ml·g^{-1}·min^{-1}	b'	100 mM
P_0X_T	10 μmol·g^{-1}·min^{-1}	$b''(0)$	0 mM
K_1	20 mM^2	s',s''	0 mM
W	3 ml·g^{-1}	P_W	0 cm·min^{-1}·mosM^{-1}
a_1'	0.1 mM	P_{D1}	0 ml·g^{-1}·min^{-1}
$a_1''(0)$	0 mM	r	1
		α	1

the tracer and the solute may behave differently. This fact may be appreciated by looking at Fig. 1, reporting the simulation of a countertransport experiment, where the inside initial concentration of the solute is 10-fold higher than the external one. In this case an 'overshoot' of the tracer (curve T) is seen in the absence of any gradient of the driver ion and is due to the inhibition, exerted by the solute present inside the vesicle, on the tracer efflux. A gradient of the driver ion is instead necessary to obtain an accumulation of the cold solute inside the vesicle (Ref. 2, Fig. 1). In fact in the experimental condition of Fig. 1 we observe only a monotonic decrease of a_1'' (curve S). Remark that, by Eqn. 14, the ratio between unidirectional tracer fluxes gives

$$\left(\{{}^*a_1'(b')^{n_1}[\mu^{n_1/2}K_2 + a_2''(b'')^{n_2}\alpha_2\mu^{(n_1-n_2)/2}] + [{}^*a_1'(b')^{n_1}a_1''(b'')^{n_1}]\}\right)$$

$$\left(\{{}^*a_1''(b'')^{n_1}[\mu^{-n_1/2}K_2 + a_2'(b')^{n_2}\alpha_2\mu^{(n_2-n_1)/2}] + [{}^*a_1''(b'')^{n_1}a_1''(b')^{n_1}]\}\right)^{-1}$$

When only one solute is present and $b' = b'' = 1$, so that $\mu = 1$, the ratio becomes, by Eqn. 15, that given by Heinz for the tracer coupling in facilitated diffusion for a binary complex (Ref. 7, p. 50).

Conversely, if initially there is not solute inside the vesicles, the third term in square brackets in the numerator of Eqn. 14 vanishes since the specific activities of the tracer in $'$ and $''$ are equal, so that $a_1''/a_1' = {}^*a_1''/{}^*a_1'$ during the time course. For this reason the ordinates of Figs. 2a, 3, 4, 5 and 8 represent both the distribution ratios of tracers and solutes.

By taking the parameter values concerning both solutes 1 and 2 equal, and substituting in Eqn. 13, one finds

$$J_1 = \alpha_1 P_0 X_T \{a_1'(b')^{n_1}[\mu^{n_1/2}K_2 + a_2''(b'')^{n_2}\alpha_2] - a_1''(b'')^{n_1}[\mu^{-n_1/2}K_2 + a_2'(b')^{n_2}\alpha_2]\}/\{\}^{00}$$

where the numerator is the same as in Eqn. 15, when allowance is made that $K_1 = K_2$, ${}^*a_1 = a_1$, $a_1 = a_2$, $\alpha_1 = \alpha_2$ and $n_1 = n_2$, and $\{\}^{00} \to \{\}^0$ for vanishing values of the tracer concentrations. In other words, one sees that the tracer flux appears to be that of a second solute with the same characteristics as the first one and vanishing concentrations.

The effect of water flux is shown in Fig. 2. In Fig. 2a one sees different uptake curves plotted for two different membrane water permeabilities: $P_W = 10^{-7}$ cm·min^{-1}·mosM^{-1}, $P_W = 10^{-6}$ cm·min^{-1}·mosM^{-1}. These values are of the same order of magnitude as those measured by Van Heeswijk and Van Os [8] in the brush-border membrane vesicles of the rat. We take an initial vesicular radius $r_v(0) = 0.25$ μm. The computer simulation shows that the occurrence of the peak time is anticipated with respect to $P_W = 0$ cm·min^{-1}·mosM^{-1}. In Fig. 2b the corresponding per cent changes of vesicular radius are plotted. Osmotic flux changes the vesicular volume, which decreases as water permeability increases. Compare our figure with Fig. 3 of [2] to see how peak occurrence is delayed by increasing W.

The presence of a second external solute sharing the same transport system of the first one induces a certain inhibition, due to an increased competition between isotope and solutes for the same carrier. The uptake inhibition increases with the second solute affinity for the carrier. Fig. 3 shows the interactions of two external solutes sharing the same carrier. The curve marked by (1) in which only one solute is present is shown for comparison and is the same given by Heinz and Weinstein [2] in their Fig. 1. In curve (2) the two external solutes have equal transport parameters; in this case the inhibition is simply due to an increasing concentration of the external solute. In curve (3) the second external solute has an increased affinity for the carrier.

The upper curve (4) of Fig. 3 shows the effect of an electrical potential generated by the diffusion of a bi-

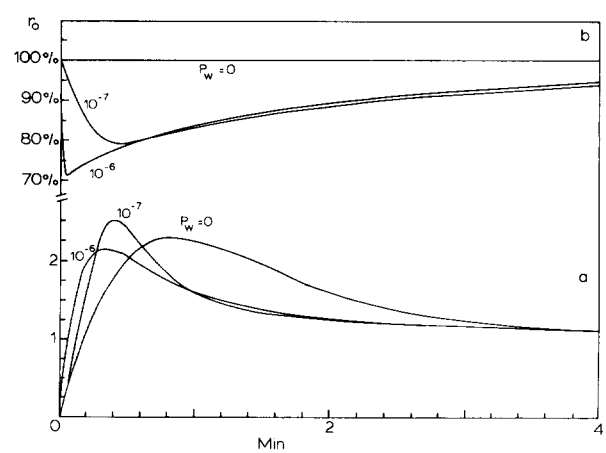

Fig. 2. (a) Uptake curves for different osmotic water permeabilities: $P_w = 0$, 10^{-7}, 10^{-6} cm·min^{-1}·mosM^{-1}; (b) relative change in the vesicular radius size for the corresponding values of osmotic water permeability when $r_v(0) = 0.25$ μm. The other parameter values are given in Table I, except for $s' = s'' = 100$ mM.

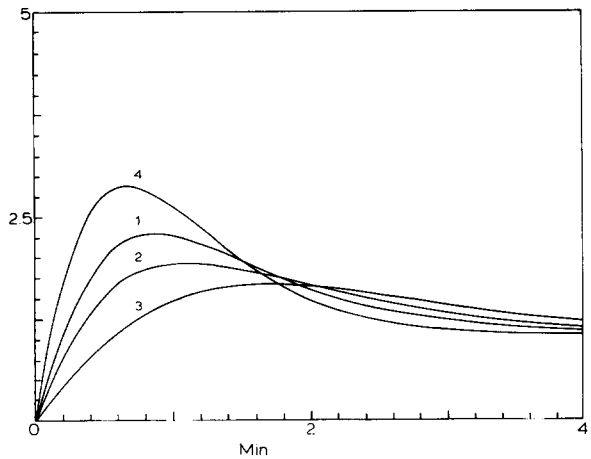

Fig. 3. Effect of electrical potential difference and interaction of a second external solute on the uptake curves: (1) $a_2' = a_2''(0) = 0$; (2) effect of the second solute $a_2' = 0.1$ mM, $a_2''(0) = 0$, with the same parameter values as the first one (Table I); (3) effect of a second solute $a_2' = 0.1$ mM, $a_2''(0) = 0$, with $K_2 = 5$ mM^2; (4) effect of electrical potential difference ($r = 0.2$, uncharged carrier, $a_2' = a_2''(0) = 0$). The parameter values not explicitly indicated are given in Table I.

nary salt with $r = 0.2$, calculated according to Goldman and Hodgkin equation.

In Fig. 4 a countertransport simulation is shown, when the vesicles are preloaded with a second solute a_2'' with the same ($K_2 = 20$ mM^2) or different affinities ($K_2 = 5$ and 40 mM^2, respectively) for the carrier. Observe that now the rate of uptake and the overshoot increase with the second solute affinity for the carrier, due to a greater inhibition exerted on the tracer efflux. The curve $K_2 = 20$ mM^2 is the same one (on a different ordinate axis) marked by (T) in Fig. 1.

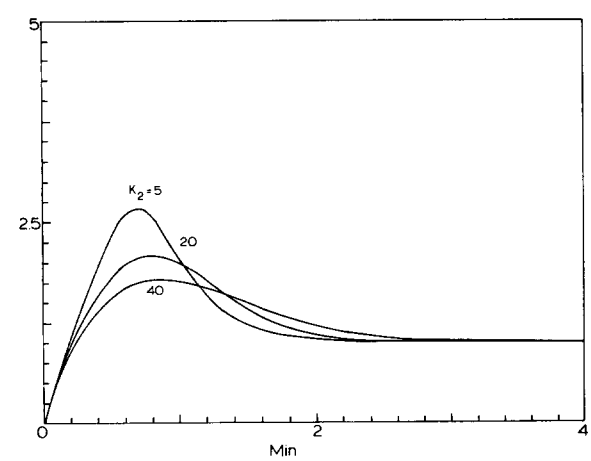

Fig. 4. Interaction of different internal solutes on countertransport uptake curves when the internal (second) solute has the same affinity for the carrier as the external (first) solute ($K_2 = 20$ mM^2), an increased affinity ($K_2 = 5$ mM^2) or a decreased one ($K_2 = 40$ mM^2); in all cases $a_2'(0) = 0$ mM, $a_2'' = 1$ mM, $b''(0) = 100$ mM, $\alpha_2 = \alpha_1 = 1$, $n_2 = n_1 = 1$, the other parameter values as in Table I.

A further extension of the model to the case of a non symmetric membrane may be considered. The results restricted to the case of one solute and its tracer are given below. By taking into account the detailed balance relation (see, for example, Ref. 7, p. 38) $P'P_0''K'' = P''P_0'K'$, and following a procedure similar to that outlined above, one obtains

$$J = P''P_0'P_0''X_T\{[a'(b')^n\mu^{n/2} - a''(b'')^n\mu^{-n/2}]K'K''\}/\{\} \quad (16)$$

and

$$*J = P''P_0'P_0''X_TK'K''\{[*a'(b')^n\mu^{n/2} - *a''(b'')^n\mu^{-n/2}] + (P''/(P_0''K''))[*a'(b')^na''(b'')^n - *a''(b'')^na'(b')^n]\} /\{\} \quad (17)$$

where

$$\{\} = P_0''K'(K'')^2(P_0' + P_0'') + a'(b')^nK''(K''(P_0'')^2 + P''P_0'K'\mu^{n/2}) + a''(b'')^n[P_0''K'K''(P_0' + P''\mu^{-n/2}) + P''(P_0'K'\mu^{n/2} + P_0''K''\mu^{-n/2})a'(b')^n]$$

Indexes 1 and 2 have been suppressed according to the fact that only one solute is present.

When $P_0' = P_0'' = P_0$, $P'' = \beta P_0$, Eqns. 16 and 17 yield, respectively,

$$J = K'K''\beta P_0X_T[a'(b')^n\mu^{n/2} - a''(b'')^n\mu^{-n/2}]/[*] \quad (18)$$

$$*J = K'\beta P_0X_T\{[*a'(b')^n\mu^{n/2} - *a''(b'')^n\mu^{-n/2}]K'' + [*a'(b')^na''(b'')^n - *a''(b'')^na'(b')^n]\beta\}/[*] \quad (19)$$

where

$$[*] = 2K'(K'')^2 + a'(b')^nK''(K'' + \beta K'\mu^{n/2}) + a''(b'')^n[K'K''(1 + \mu^{-n/2}\beta) + \beta a'(b')^n(K'\mu^{n/2} + K''\mu^{-n/2})]$$

Fig. 5 shows the effect of some asymmetries in the dissociation constants of the ternary complex, by making use of the preceding calculations. Observe that, increasing the solute affinity for the carrier on the internal side of the membrane ($K'' = 10$ mM^2), the peak height increases and anticipates, while it decreases and is delayed when the affinity is reduced ($K'' = 40$ mM^2).

When $K' = K'' = K$, $P_0' = P_0'' = P_0$, Eqns. 16 and 17 reduce to Eqn. A6-a of Ref. 2 and to Eqn. 15 in this paper.

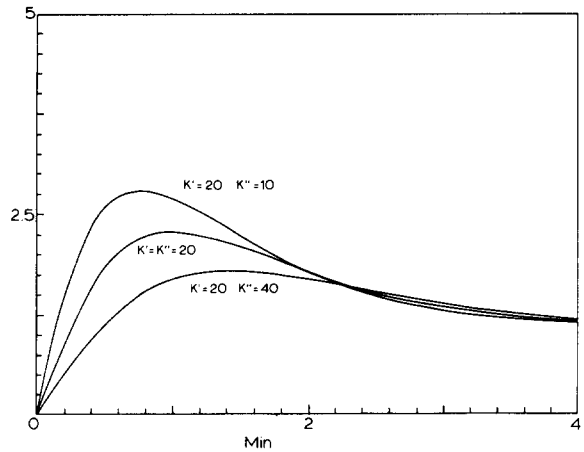

Fig. 5. Effect of an asymmetric membrane on the uptake curves: ($K' = 20$, $K'' = 20$) equal affinity on both side of the membrane; ($K' = 20$, $K'' = 10$) increased affinity on the internal side of the membrane vesicles; ($K' = 20$, $K'' = 40$) decreased affinity on the internal side of the membrane vesicles. The other parameters are given in Table I.

To take into account the presence of the tracer specifically bound to the membrane, one should also consider the terms giving the quantity of tracer making ternary complexes at the two sides of the vesicular membrane, since ${}^*B_i = (a_i b^{n_i} x)' + (a_i b^{n_i} x)''$.

For non symmetric membranes and $P_0' = P_0'' = P_0$, taking into account that

$${}^*(ab^n x)' = (ab^n x)'({}^*a'/a') = {}^*a'(b')^n x'/K'$$

one finds

$${}^*(ab^n x)' = X_T[(K''\beta a''(b'')^n \mu^{-n/2} + (K'')^2){}^*a'(b')^n]/[{}^*] \quad (20)$$

In a similar way one obtains

$${}^*(ab^n x)'' = X_T[(K'\beta a'(b')^n \mu^{n/2} + K'K''){}^*a''(b'')^n]/[{}^*] \quad (21)$$

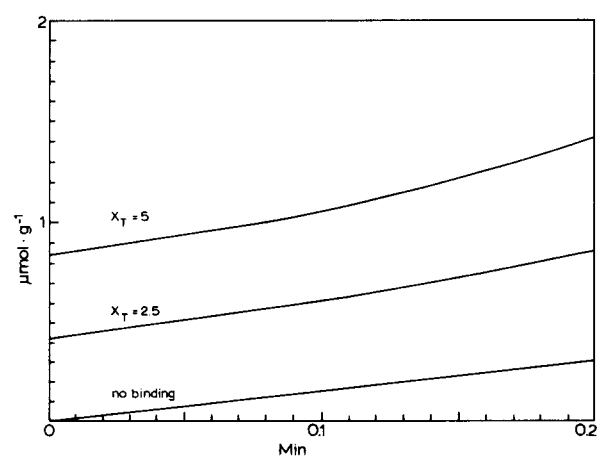

Fig. 6. Effect of the solute binding to the membrane on its initial uptake values. On the ordinate is the internal solute quantity per gram of membrane protein. If no binding is considered, the initial uptake value is null, while in its presence it increases with X_T (2.5 or 5 μmol·g^{-1}). The other parameters are given in Table I.

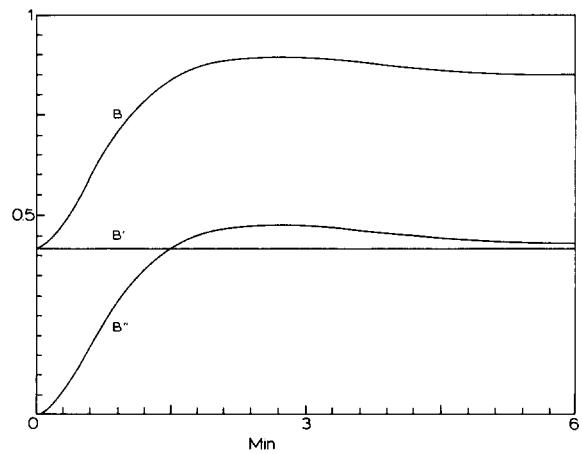

Fig. 7. Different contributions of internal (B'') and external (B') components of the binding to the total binding (B) for $X_T = 2.5$ μmol·g^{-1}. The other parameters are given in Table I.

Observe that what is important for binding is the parameter X_T, instead of the block $P_0 X_T$ appearing in the preceding equations regarding fluxes.

Fig. 6 shows, on an enlarged time scale, the effect of solute binding on uptake values, for two different values of X_T, compared with the case when no binding is considered. The initial value of the binding is given by the zero time intercept on the ordinate axis. Observe how the effect increases with the total amount of carrier species present in the membrane. In this figure and in the following one the values of the ordinate axis have been multiplied by $a'/{}^*a'$, as it is customary in the experimental measure of fluxes by means of tracers.

In Fig. 7 the binding time course ($X_T = 2.5$ μmol·g^{-1}) has been split in its internal (B'') and external (B') components and plotted on a different time scale. Observe that in this case ($\beta = 1$) only the internal binding changes during the time course, while the external binding remains constant. For other values of β or when electrical potential effects are considered, also the external binding may vary during the time course.

Appendix

Here we want to check to what extent the assumption regarding the speed of carrier distribution holds. We consider for the sake of brevity, only the case of one solute and a symmetric membrane, so that index i may be suppressed. In this case instead of Eqn. 8a one has

$$dx'/dt = P(ab^n x)'\mu^{n/2} + P_0 x' - P(ab^n x)''\mu^{-n/2} - P_0 x'' \quad (A\text{-}1)$$

By taking into accounts Eqns. 6 and 7, Eqn. A-1 becomes

$$-dx'/dt = [Pa'(b')^n \mu^{n/2} x'/K + P_0 x' - Pa''(b'')^n \mu^{-n/2} x'' /K - P_0 x'']/\{\} \quad (A\text{-}2)$$

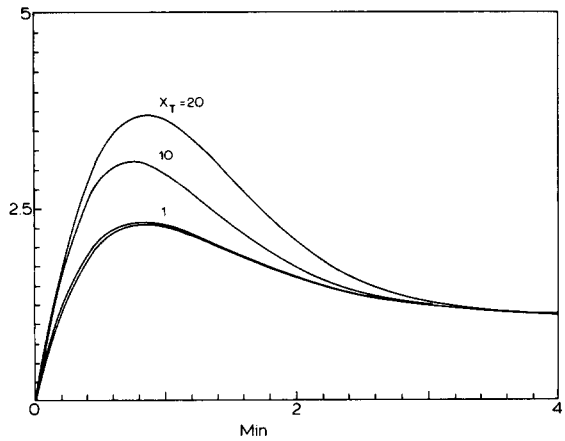

Fig. 8. Effect of the carrier species net flux on solute uptake for increasing values of X_T: 1 μmol·g^{-1}, 10 μmol·g^{-1}, 20 μmol·g^{-1}; the lower curve is calculated assuming null net translocation of the carrier species. The values of the other parameters are given in Table I.

where

$$x'' = [X_T - x'[1 + a'(b')^n/K]/[1 + a''(b'')^n/K]$$

$$\{\} = [1 + a''(b'')^n/K]/[1 + a'(b')^n/K]$$

The differential Eqn. A-2 has to be integrated with

$$d/dt(Wa'') = P[a'(b')^n\mu^{n/2}x/K - a''(b'')^n\mu^{-n/2}x''/K] \quad \text{(A-3)}$$

The initial condition $x'(0)$ may be found taking into account that internal and external solutes and carrier species are equilibrated before the beginning of a transport experiment, so that

$$2x'(0) + 2a''(0)b''(0)x'(0)/K = X_T \quad \text{(A-4)}$$

Fig. 8 presents the results of the numerical integration of system A-2 and A-3, subject to initial conditions $a''(0) = 0$ and Eqn. A-4. For low values of X_T, no difference appears between the present integration and that presented above. Conversely, for values of X_T higher than 1 μmol · g^{-1}, an increasing effect due to the net flux of carrier species across the membrane has to be taken into account. In this case the assumption expressed by Eqn. 8a is no longer acceptable.

Acknowledgements

The authors are indebted with Dr. B. Giordana and Dr. G. Hanozet who first drew attention to the problem, for criticism and several helpful discussions.

References

1 Weiss, S.D., McNamara, P.D. and Segal, S. (1981) J. Theor. Biol. 93, 597–608.
2 Heinz, E. and Weinstein, A.M. (1984) Biochim. Biophys. Acta 776, 83–91.
3 Turner, R.J. (1981) Biochim. Biophys. Acta 649, 269–280.
4 Turner, R.J. and Silverman, M. (1980) Biochim. Biophys. Acta 596, 272–291.
5 Hopfer, U. and Groseclose, R. (1980) J. Biol. Chem. 255, 4453–4462.
6 Läuger, P. (1980) J. Membr. Biol. 57, 163–178.
7 Heinz, E. (1978) Mechanics and Energetics of Biological Transport, Springer, Berlin.
8 Van Heeswijk, M.P.E. and Van Os, C.H. (1986) J.Membr. Biol. 92, 183–193.